Bioresource Technology 153 (2014) 340–350

Contents lists available at ScienceDirect

Bioresource Technology

journal homepage: www.elsevier.com/locate/biortech

Comprehensive modeling and investigation of the effect of iron on the growth rate and lipid accumulation of *Chlorella vulgaris* cultured in batch photobioreactors

Alessandro Concas [a,*], Alberto Steriti [b], Massimo Pisu [a], Giacomo Cao [a,b,c,*]

[a] Center for Advanced Studies, Research and Development in Sardinia (CRS4), Loc. Piscina Manna, Building 1, 09010 Pula (CA), Italy
[b] Research Unit of the National Interuniversity Consortium "The Chemistry for the Environment", Interdepartmental Center of Environmental Science and Engineering (CINSA), University of Cagliari, Via San Giorgio 12, 09124 Cagliari, Italy
[c] Department of Mechanical, Chemical and Materials Engineering, University of Cagliari, Piazza d'Armi, 09123 Cagliari, Italy

HIGHLIGHTS

- A comprehensive model describing the effect of iron on lipid production of C. Vulgaris is proposed.
- Model results are successfully compared with experimental data.
- The model might allow to optimize iron-based strategies to improve the lipid productivity of algae.

ARTICLE INFO

Article history:
Received 4 October 2013
Received in revised form 26 November 2013
Accepted 30 November 2013
Available online 8 December 2013

Keywords:
Mathematical modeling
Effect of iron
Microalgae
Lipid accumulation
Biofuels

ABSTRACT

Recent works have shown that specific strains of microalgae are capable to simultaneously increase their growth rate and lipid content when cultured under suitable concentrations of iron. While these results are promising in view of the exploitation of microalgae for producing biofuels, to the best of our knowledge, no mathematical model capable to describe the effect of iron on lipid accumulation in microalgae, has been so far proposed. A comprehensive mathematical model describing the effect of iron on chlorophyll synthesis, nitrogen assimilation, growth rate and lipid accumulation in a freshwater strain of *Chlorella vulgaris* is then proposed in this work. Model results are successfully compared with experimental data which confirm the positive effect of growing iron concentrations on lipid productivity of *C. vulgaris*. Thus, the proposed model might represent a useful tool to optimize iron-based strategies to improve the lipid productivity of microalgal cultures.

1. Introduction

The potential exploitation of microalgae as renewable resource for the production of biofuels is receiving a rising interest mostly driven by the global concerns related to the depletion of fossil fuels supplies and the increase of CO_2 levels in the atmosphere. In spite of such interest, the existing microalgae-based technology for CO_2 sequestration and biofuels production is still not widespread since it is affected by economic and technical constraints that might have limited the development of industrial scale production systems. Therefore, in view of industrial scaling-up, the current technology should be optimized in terms of lipid productivities as well as design/operating parameters. The identification of the optimal design and operating parameters that allow the existing strains to increase their lipid content while maintaining an high growth rate, may be accomplished by exploiting suitable process engineering techniques (Concas et al., 2010, 2012). Among them, the most widespread one consists of the induction of nitrogen starvation phenomena in the culture (Sharma et al., 2012; Concas et al., 2013). In fact, under starvation conditions, nitrogen concentration is not enough for activating the metabolic pathways leading to protein synthesis required by algal growth so that the excess of carbon due to photosynthesis is channeled into storage molecules such as triacylglycerides or starch (Scott et al., 2010). However, while from one hand such phenomenon can lead to increase the lipid content, on the other one it results in lower growth rates of microalgae since fundamental proteins cannot be synthesized. Beside nitrogen starvation, several methods are currently being investigated for the induction of lipid biosynthesis in microalgae. Specifically these

* Corresponding authors. Tel.: +39 070 9250352; fax: +39 070 9250216 (A. Concas and G. Cao). Address: Center for Advanced Studies, Research and Development in Sardinia (CRS4), Loc. Piscina Manna, Building 1, 09010 Pula (CA), Italy.
E-mail addresses: aconcas@crs4.it (A. Concas), giacomo.cao@dimcm.unica.it (G. Cao).

0960-8524/$ - see front matter © 2013 Elsevier Ltd. All rights reserved.
http://dx.doi.org/10.1016/j.biortech.2013.11.085

Notations

[EDTA] total molar concentration of EDTA not bound to iron species ($mol_{EDTA}\ m^{-3}$)
[Fe(II)] total molar concentration of dissolved inorganic species of reduced iron ($mol_{Fe}\ m^{-3}$)
[Fe(III)] total molar concentration of dissolved inorganic species of oxidized iron ($mol_{Fe}\ m^{-3}$)
[Fe(III) – EDTA] total molar concentration of species of oxidized iron bound to EDTA ($mol_{Fe}\ m^{-3}$)
C_b total biomass concentration which accounts for both lipidic and non lipidic fraction ($g_{dw}\ m^{-3}$)
$C_{Fe(III)}$ total mass concentration of Fe(III) in bulk phase, MW_{Fe} [Fe(III)] ($g_{Fe}\ m^{-3}$)
C_ℓ concentration of the lipidic fraction of algal biomass ($g_{dw}\ m^{-3}$)
C_N total mass concentration of N species in bulk phase ($g_N\ m^{-3}$)
C_x concentration of non lipidic fraction of algal biomass ($g_{dw}\ m^{-3}$)
I_0 incident light intensity ($\mu E\ m^{-2}\ min^{-1}$)
$\bar{I}$ average light intensity within an infinitesimal cylinder ($\mu E\ m^{-2}\ min^{-1}$)
I_{av} average light intensity within the culture ($\mu E\ m^{-2}\ min^{-1}$)
k_d rate constant for Fe(III)–EDTA dissociation (min^{-1})
k_f rate constant for Fe(III) chelation by EDTA ($m^3\ mol^{-}\ min^{-1}$)
$k_{h\nu}$ rate constant for the photolytic dissociation of Fe(III)–EDTA (min^{-1})
k_{ox} rate constant for Fe(II) oxidation (min^{-1})
K_{Fe} half saturation constant of iron ($g_{Fe}\ m^{-3}$)
K_N half saturation constant of nitrogen ($g_N\ m^{-3}$)
MW_{Fe} molecular weight of iron ($g_{Fe}\ mol_{Fe}^{-1}$)
MW_N molecular weight of nitrogen ($g_N\ mol_N^{-1}$)
P carbon-specific photosynthetic rate (net carbon fixation rate) ($g_C\ g_{dw}^{-1}\ min^{-1}$)
P_c^{max} carbon-specific maximum photosynthetic rate ($g_C\ g_{dw}^{-1}\ min^{-1}$)
P_c^{sat} carbon-specific light-saturated photosynthetic rate ($g_C\ g_{dw}^{-1}\ min^{-1}$)
q_{Chla} chlorophyll-a cell quota ($g_{Chla}\ g_{dw}^{-1}$)
q_{Chla}^0 initial chlorophyll-a cell quota ($g_{Chla}\ g_{dw}^{-1}$)
q_{Fe} iron cell quota ($g_{Fe}\ g_{dw}^{-1}$)
q_{Fe}^0 initial iron quota ($g_{Fe}\ g_{dw}^{-1}$)
Q_{Fe}^{max} maximum iron cell quota above which iron uptake is stopped ($g_{Fe}\ g_{dw}^{-1}$)
Q_{Fe}^{min} minimum iron cell quota under which growth is inhibited ($g_{Fe}\ g_{dw}^{-1}$)
q_ℓ lipid cell quota ($g_{dw}\ g_{dw}^{-1}$)
q_ℓ^0 initial lipid quota ($g_{dw}\ g_{dw}^{-1}$)
q_N nitrogen cell quota ($g_N\ g_{dw}^{-1}$)
q_N^0 initial nitrogen quota ($g_N\ g_{dw}^{-1}$)
Q_N^{max} maximum nitrogen cell quota above which nitrogen uptake is stopped ($g_N\ g_{dw}^{-1}$)
Q_N^{min} minimum nitrogen cell quota under which growth is inhibited ($g_N\ g_{dw}^{-1}$)
T_P photoperiod (min)
v_{Fe} Iron uptake rate ($g_{Fe}\ g_{dw}^{-1}\ min^{-1}$)
v_{Fe}^{max} maximum iron uptake rate ($g_{Fe}\ g_{dw}^{-1}\ min^{-1}$)
v_N nitrogen uptake rate ($g_N\ g_{dw}^{-1} min^{-1}$)
v_N^{max} maximum nitrogen uptake rate ($g_N\ g_{dw}^{-1}\ min^{-1}$)
z vertical axis of flasks or bottles (m)

Greek letters

α rate of primary production of lipids ($g_{dw}\ g_{dw}^{-1}$)
β initial slope of the iron-dependent photosynthesis irradiance (P–I) curve ($g_C\ m^2\ g_{Chla}^{-1}\ \mu E^{-1}$)
χ carbon content of non-lipid fraction of microalgae ($g_C\ g_{dw}^{-1}$)
γ_{Fe} hyperbolic function describing the effect of iron on nitrogen uptake rate (–)
γ_N linear function of nitrogen cell quota (–)
η rate of secondary (iron induced) production of lipids ($g_{dw}\ g_{dw}^{-1}\ min^{-1}$)
η_m maximum rate of secondary (iron induced) production of lipids ($g_{dw}\ m^3\ g_{dw}^{-1}\ min^{-1}\ g_{Fe}^{-1}$)
μ specific growth rate of the non-lipid fraction of microalgae (min^{-1})
μ_{max} maximum specific growth rate of the non-lipid fraction of microalgae (min^{-1})
θ_{Chla}^N weight of chloropyll synthesized for unit weight of nitrogen assimilated ($g_{Chla}\ g_N^{-1}$)
$\theta_{Chla}^{N,max}$ maximum amount of chloropyll synthesized for unit weight of nitrogen assimilated ($g_{Chla}\ g_N^{-1}$)
τ_a optical extinction coefficient for biomass ($m^2\ g^{-1}$)
ω angle of incidence of light (rad)

Subscripts

b total biomass which accounts both lipid and non-lipid fraction (–)
c carbon specific value (–)
Chla chlorophyll-a (–)
ℓ lipid fraction of biomass (–)
x non lipid fraction of biomass (–)

Superscripts

0 initial value (–)
f final value (–)
max maximum value (–)
min minimum value (–)
tot total value (–)

techniques are based on cultivating algae under extreme pH and temperature conditions, high radiation, osmotic stress, and high heavy metals concentration (Sharma et al., 2012). All these methods have in common process conditions that lead the microalgal cells to use the carbon assimilated through photosynthesis for synthesizing lipids rather than proteins or other structural molecules. In fact, lipids in the form of triacylglycerides provide a storage function that enables microalgae to endure adverse environmental conditions (Sharma et al., 2012). Nevertheless, the side effect of all the techniques above is the lowering of microalgae growth rate. Therefore, similarly to what happen with nitrogen starvation, while from one side the lipid content of microalgae is increased, on the other hand the growth rate is correspondingly reduced and thus the global lipid productivity achieved is similar to the one which might be obtained by cultivating algae under normal conditions. For this reason the identification of suitable operating conditions that allow to increase at the same time both lipid content and biomass growth rate is one of the main challenges in the field of biofuels production through microalgae.

Among the micronutrients which can improve microalgae growth rate, iron is well known to be one of the most important. In fact, such component is vital for microalgae metabolism, since it represents a constituent of the cytochrome b6-f complex which is an enzyme found in the thylakoid membrane of chloroplasts of

green algae that mediates the transfer of electrons from Photosystem II to Photosystem I. Moreover, iron limitation affects the synthesis of phycocyanin and chlorophyll. Finally, the redox properties of iron are critical for nitrogen assimilation and fixation, photosynthesis, respiration and DNA synthesis. Ultimately, iron limitation can result in the reduction of the rate of CO_2 fixation and inorganic nitrogen assimilation of phytoplankton by limiting the light reactions of photosynthesis (Buitenhuis and Geider, 2010).

Liu et al. (2008) have shown that an increasing of bio-available iron concentration in the growth medium can lead to a simultaneous increase of both lipid content and growth rate of a marine strain of *Chlorella vulgaris*. Specifically when the initial iron concentration in the growth medium is increased from 0 to 1.2×10^{-5} - mol L^{-1}, a corresponding increase in the lipid content from 7.8% to 57% by weight of dry biomass could be observed. While such results have not been so far quantitatively confirmed in the literature, from a qualitative point of view a similar behavior has been observed by Ruangsomboon (2012) when considering *Botryococcus braunii*. Specifically, it was observed that, while biomass growth rate was not significantly affected by initial iron concentration, the corresponding lipid content markedly increased from 22% to 35% by dry weight when the initial iron concentration is correspondingly augmented from 9 to 27 mg L^{-1}. Similar results were obtained by Ruangsomboon et al. (2013) when considering the green alga Scenedesmus dimorphus whose lipid content greatly increased when the initial iron concentration was augmented from 9 to 47 mg L^{-1}. Specifically, a maximum lipid content of about 24.7% was observed for Scenedesmus dimorphus when it was cultivated under the maximum initial concentration of iron considered (i.e. 47 mg L^{-1}). Baky et al. (2012) reported that the accumulation of total lipids shows an increasing trend when Fe^{3+} concentrations in solution was augmented up to 20 mg L^{-1}. Recently, Mata et al. (2013) demonstrated that by increasing the Fe concentration in the culture medium 10 times with respect to the base case, the maximum lipid productivity of Dunaliella tertiolecta increased to almost the double, correspondingly. Finally, Yeesang and Cheirsilp (2011) reported that high level of iron improved lipid accumulation in four different strains of microalgae. Ultimately, the experimental results summarized above seem to confirm that when the initial iron concentration is increased within a specific range, a simultaneous augmentation of growth rate and lipid content can be observed for specific strains. While these results are promising in the light of the microalgae technology optimization, on the other hand, to the best of our knowledge, no exhaustive explanation on how iron can influence the lipid biosynthesis in microalgae has been so far provided. Moreover, such a lack of understanding seems to have limited the development of iron based strategies to improve bio-oil yields, and hence their potential application at the industrial scale for the production of biofuels through microalgae. For these reasons further and deeper investigations about the effect of iron on lipid accumulation in microalgae are required. In this regard, while the identification of the phenomena involved needs an extremely accurate experimental research, the optimization of design and operating parameters for the application of the iron-based strategy to the industrial scale, may be accomplished by exploiting suitable process engineering techniques. To this aim, mathematical models, that are capable to quantitatively describe the influence of iron on microalgae growth and lipid accumulation, are needed (Quinn et al., 2011). To the best of our knowledge, no comprehensive simulation models, which account simultaneously for all the complex phenomena taking place during lipid accumulation in microalgae when varying iron concentration, have been so far proposed in the literature. Consequently, the goal of the present work is to propose a complete mathematical model to quantitatively describe the growth of microalgae and their lipid accumulation as a function of iron concentration in solution. In order to validate model results, specific experiments were performed with a strain of *C. vulgaris*, where the iron concentration in solution was suitably changed. It is worth noting in passing that, to the best of our knowledge, such experimental investigation deals for the first time with a freshwater strain of *C. vulgaris*.

2. Methods

2.1. Microorganism, culture conditions and culture medium

The fresh water algal strain *C. vulgaris* (Centro per lo Studio dei Microorganismi Autotrofi, CNR, Florence, Italy) was considered in this work. Unialgal stock cultures were propagated and maintained in Erlenmeyer flasks with a Kolkwitz Triple Modified (KTM-A) medium under incubation conditions of 25 °C, a photon flux density of 98 μE m^{-2} s^{-1} provided by four 15 W white fluorescent tubes, and a light/dark photoperiod of 12 h. Flasks were continuously shaken at 100 rpm (Universal Table Shaker 709).

Growth experiments were performed in Erlenmeyer flasks and Pyrex bottles under axenic conditions. The culture media volumes were 250 mL and 1 L for flasks and bottles, respectively, which were agitated by a magnetic stirrer at 300 rpm using magnetic PFTE stir bars (6 mm diameter and 30 mm length). Flasks, bottles, and magnetic stir bars, as well as culture media were sterilized in autoclave at 121 °C for 20 min prior to microalgae inoculation. Either flasks or bottles were stoppered by means of cotton plugs wrapped in cotton gauze during cultivation in order to prevent external contamination while at the same time assuring atmospheric CO_2 diffusion within the culture. Algae were cultured at room temperature and under a photon flux density of 100 μE m^{-2} - s^{-1} provided by six 11 W white fluorescent tubes and a light/dark photoperiod of 12 h. The initial cell concentration in each experiment varies from 0.065 to 0.088 g L^{-1}.

The culture medium consisted of a modified Kolkwitz medium (KTM-A) containing 2.5 g L^{-1} of KNO_3, 0.5 g L^{-1} of KH_2PO_4, 0.27 g L^{-1} of $MgSO_4 \cdot 7H_2O$, 0.04 g L^{-1} of $CaCl_2 \cdot 2H_2O$, 1 g L^{-1} of $NaHCO_3$ and 1 mL of micronutrients solution The latter one contained 2.86 g L^{-1} of H_3BO_3, 1.81 g L^{-1} of $MnCl_2 \cdot 7H_2O$, 0.222 g L^{-1} of $ZnSO_4 \cdot 7H_2O$, 0.035 g L^{-1} of $CoCl_2 \cdot 6H_2O$, 0.080 g L^{-1} of $CuSO_4 \cdot 5H_2O$, and 0.230 g L^{-1} of $Na_2MoO_4 \cdot 2H_2O$. Iron was supplied in chelated form by adding to the culture medium suitable volumes from a solution containing 29.75 g L^{-1} of $Na_2EDTA \cdot 2H_2O$ and 24.90 g L^{-1} of $FeSO_4 \cdot 7H_2O$, respectively. Specifically, *C. vulgaris* was cultivated in the above specified medium supplemented with $FeSO_4 \cdot 7H_2O$ at the iron concentration levels equal to 0.0, 1.8×10^{-1}, 4.5×10^{-1} and 1.8 mol m^{-3} or 0.0, 10.0, 25.0 and 100 g m^{-3} corresponding to $Na_2EDTA \cdot 2H_2O$ concentrations of 0.0, 1.6×10^{-1}, 4.0×10^{-1} and 1.6 mol m^{-3}, respectively.

2.2. Biomass and pH measurement

The growth of microalgae was monitored through spectrophotometric measurements (Genesys 20 spectrophotometer, Thermo Fisher Scientific Inc. Waltham) of the culture media optical density (OD) at 560 nm wavelength (D_{560}) with 1 cm light path. Specifically, 1 mL of culture medium was withdrawn under clean bench at each time point and was subjected to spectrophotometric analysis performed under clean bench using sterilized cuvettes to avoid bacterial contamination. Subsequently, the volume of culture withdrawn for analysis was re-inserted in the flasks in order to avoid changes in the culture volume. The biomass concentration C_b (g_{dw} L^{-1}) was calculated from OD measurements using a suitable C_b vs. OD calibration curve which was obtained by gravimetrically evaluating the biomass concentration of known culture medium volumes that were previously centrifuged at 4000 rpm for 15 min

and dried at 105 °C for 24 h. The pH was daily measured by pH-meter (KNICK 913). For the sake of reproducibility, each experimental condition was repeated at least twice. The average and standard errors values of the experimental results were calculated by taking advantage of OriginPro 8 software.

2.3. Lipid extraction

In order to evaluate the lipid content of *C. vulgaris*, the microalgae were first harvested and then centrifuged to obtain a wet biomass pellet characterized by a humidity of about 90%wt./wt. Lipid extraction was performed directly on wet biomass. The method proposed by Molina Grima et al. (1994) was adopted for extracting lipids from microalgae through direct saponification. Briefly it consists in contacting suitable amounts of wet micro-algal biomass with an extraction/saponification solution prepared by dissolving 2.16 g of KOH in 100 mL of ethanol (96% purity). Specifically, 1 g of wet biomass was contacted for 8 h with 6 mL of the solution above in a stirred flask at room temperature. Unsaponifiables were then separated by five extractions with 2 mL of hexane. In order to shift the equilibrium distribution of unsaponifiables to the hexane phase, 1 mL of water was added. The hydroalcoholic phase containing soaps, was then acidified by adding HCl in a 1:1 volumetric ratio in order to obtain a pH of about 1. The lipids obtained were then recovered through eight extractions with 2 mL hexane and subsequently weighted. By dividing the weight of lipids obtained and the initial dry weight of the biomass which underwent the extraction procedure, the lipid content of microalgae, q_ℓ was evaluated. It is noteworthy to mention here that when microalgae were cultivated in absence of dissolved iron, their lipid content q_ℓ^0 at the start of the cultivation was equal to the corresponding one measured at the end, q_ℓ^f.

3. Mathematical modeling

As shown in the experimental section iron is added to the growth medium as $FeSO_4{\cdot}7H_2O$ mixed with suitable amount of $Na_2EDTA{\cdot}2H_2O$. Several reactions taking place in solution are capable to allocate iron in different molecular species or complexes. In fact, iron in solution can exist in two oxidation states, Fe(III) or Fe(II) as well as in the form of free ion or complexed with inorganic or organic ligands. Some of the iron species formed can be uptaken by microalgae while some others cannot. Therefore, it is important to simulate complexation and chelation phenomena occurring in solution in order to evaluate the concentration of iron species that are available for microalgae metabolism. In water solution, $FeSO_4$ and Na_2EDTA are able to dissociate and release Fe^{2+} and EDTA ions. The Fe^{2+} ions in water solution can react with OH^- ions to form inorganic complexes among which the most relevant are $Fe(OH)^+$, $Fe(OH)_2$ and $Fe(OH)_3^-$ (Millero et al., 1995). However, at pH values close to neutrality, the main ionic form of reduced iron is just Fe^{2+} free ion that is quickly oxidized to Fe^{3+} (Morgan and Lahav, 2007). Subsequently, Fe^{3+} ions are involved in a number of reactions with OH^- ions which lead to the formation of the Fe^{3+} inorganic complexes shown in Table 1. Both Fe^{3+}free ions and Fe^{3+}inorganic complexes can be then chelated by EDTA ions that are in solution to form the organic complexes shown in Table 1 (Shaked et al., 2005). The relevant iron complexes which are formed as a result of the complexation–chelation phenomena taking place in solution can be thus defined as $Fe^{2+}$and Fe^{3+} free ions and inorganic complexes as well as Fe^{3+} organically chelated ones whose total concentrations will be hereafter indicated by [Fe(II)], [Fe(III)] and [Fe(III)–EDTA] respectively, as shown in Table 1. It is apparent that, given the growth medium composition, also different iron complexes can be formed by reaction with anions such as sulfates, chlorides, etc. However, according to Millero et al. (1995) their concentration is very low at the pH values that are detected during the experiments carried out in this work. Ultimately, the total concentration of the main forms of iron can be calculated as shown in what follows:

Table 1
Different iron complexes formed in a solution containing EDTA.

Inorganic and chelated Fe complexes in solution	Symbols adopted for the corresponding total concentration	References
Fe^{2+}	[Fe(II)]	Millero et al. (1995)
$Fe(OH)^+$		Millero et al. (1995)
$Fe(OH)_2$		Millero et al. (1995)
$Fe(OH)_3^-$		Morgan and Lahav (2007)
Fe^{3+}	[Fe(III)]	Millero et al. (1995)
$Fe(OH)^{2+}$		Millero et al. (1995)
$Fe(OH)_2^+$		Millero et al. (1995)
$Fe(OH)_3$		Millero et al. (1995)
$Fe(OH)_4^-$		Millero et al. (1995)
$Fe–EDTA^-$	Fe(III)–EDTA	Gerringa et al. (2000)
$Fe(OH)–EDTA^{2-}$		Gerringa et al. (2000)
$Fe(OH)_2–EDTA^{3-}$		Gerringa et al. (2000)

$$[\mathrm{Fe(II)}] = [\mathrm{Fe^{2+}}] + [\mathrm{Fe(OH)^+}] + [\mathrm{Fe(OH)_2}] + [\mathrm{Fe(OH)_3^-}] \quad (1)$$

$$[\mathrm{Fe(III)}] = [\mathrm{Fe^{3+}}] + [\mathrm{Fe(OH)^{2+}}] + [\mathrm{Fe(OH)_2^+}] + [\mathrm{Fe(OH)_3}] + [\mathrm{Fe(OH)_4^-}] \quad (2)$$

$$[\mathrm{Fe(III)-EDTA}] = [\mathrm{FeEDTA^-}] + [\mathrm{Fe(OH)EDTA^{2-}}] + [\mathrm{Fe(OH)_2EDTA^{3-}}] \quad (3)$$

In the conventional model used for simulating iron uptake by eukaryotic microalgae, the corresponding rate is proposed to depend upon the concentration of unchelated Fe(III) species (Hudson et al., 1990; Shaked et al., 2005). According to this model, iron is bound as Fe(III) species to a cell surface ligand and is subsequently transferred across the plasma membrane as schematically shown in Fig. 1 (Shaked et al., 2005). It is assumed that unchelated inorganic Fe(III) species are in chemical equilibrium with the chelate Fe(III)–EDTA through dissociation and chelation reactions whose rate constants are k_d and k_f, respectively. Upon illumination, photoreduction of Fe(III)–EDTA can also take place leading to the production of unchelated reduced iron species, i.e. Fe(II), which are in turn quickly oxidized to inorganic Fe(III). Therefore, Fe(III) represents the dominant species that are bound to cell surface ligand and are transported across the cell wall and membrane. Actually, Fe(II) species can be also captured by specific strains of algae, albeit to negligible extent (Shaked et al., 2005). As better specified in what follows, the rate of iron uptake by algae, v_{Fe} is thus proportional to the concentration of Fe(III) species. Under the assumptions above and considering the experimental conditions adopted, the relevant material balances describing the evolution of iron species in the bulk liquid phase of the experimental batch photobioreactors adopted can be thus written as follows (cf. Hudson et al., 1990):

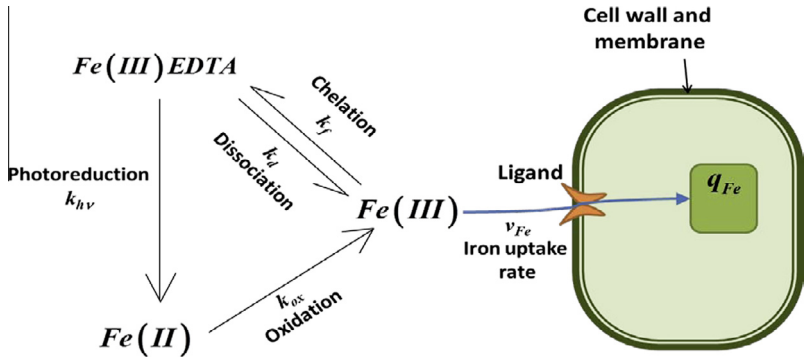

Fig. 1. Schematic representation of Fe complexation, oxidation, chelation and algal uptake phenomena occurring in solution, adapted from Hudson et al. (1990) and Shaked et al. (2005).

$$\frac{d[\mathrm{Fe(II)}]}{dt} = k_{hv}[\mathrm{Fe(III)-EDTA}] - k_{ox}[\mathrm{Fe(II)}] \tag{4}$$

$$\frac{d[\mathrm{Fe(III)}]}{dt} = k_d[\mathrm{Fe(III)-EDTA}] + k_{ox}[\mathrm{Fe(II)}] - k_f[\mathrm{Fe(III)}][\mathrm{EDTA}] - \frac{v_{\mathrm{Fe}}C_x}{MW_{\mathrm{Fe}}} \tag{5}$$

$$\frac{d[\mathrm{Fe(III)-EDTA}]}{dt} = -k_d[\mathrm{Fe(III)-EDTA}] + k_f[\mathrm{Fe(III)}][\mathrm{EDTA}] - k_{hv}[\mathrm{Fe(III)-EDTA}] \tag{6}$$

along with the corresponding initial conditions:

$$[\mathrm{Fe(II)}]^0 = [\mathrm{FeSO_4 \cdot 7H_2O}]^0 \quad \text{at} \quad t = 0 \tag{7}$$

$$[\mathrm{Fe(III)}]^0 = 0 \quad \text{at} \quad t = 0 \tag{8}$$

$$[\mathrm{Fe(III)-EDTA}]^0 = 0 \quad \text{at} \quad t = 0 \tag{9}$$

where C_x represents the concentration of the non lipidic fraction of algal biomass, while the significance of other symbols is reported in the Notation. It is important to highlight that the term [EDTA] appearing in Eqs. (5) and (6) represents the total molar concentration of EDTA ions that are not bound to Fe species (Cheize et al., 2012). The term [EDTA] thus includes both the concentration of actually free EDTA ions as well as the EDTA ions that are bound to cationic species other than iron, namely Na^+, Ca^{2+}, etc. Therefore the [EDTA] concentration can be evaluated for each cultivation time as shown in what follows (Cheize et al., 2012):

$$[\mathrm{EDTA}] = [\mathrm{EDTA}]^0 - [\mathrm{Fe(III)-EDTA}] \tag{10}$$

where:

$$[\mathrm{EDTA}]^0 = [\mathrm{Na_2EDTA \cdot 2H_2O}] \tag{11}$$

In order to simulate microalgal growth and lipid production, the following assumptions are taken into account. The microalgal cell consists of two distinct compartments, i.e. the non lipidic fraction whose concentration is indicated by C_x and the lipidic fraction whose concentration is indicated by C_ℓ. Thus, the total concentration of algal biomass, C_b is the sum of the concentrations of the two compartments. Since cultivation of microalgae has been carried out within suitable flasks operated in batch mode, the material balance for the non lipidic fraction of microalgal biomass can be written as follows (Packer et al., 2011):

$$\frac{dC_x}{dt} = \mu \cdot C_x \tag{12}$$

along with the initial condition:

$$C_x = C_x^0 \quad \text{at,} \quad t = 0 \tag{13}$$

where the symbol significance is reported in the Notation. The growth rate μ of the non lipidic fraction can be limited by nitrogen or iron concentration as well as by light intensity. Algae growth under nitrogen or iron starvation conditions are described through the well-known cell-quota model (Cherif and Loreau, 2010). On the other hand, when light intensity is the main limiting factor, the growth rate of microalgae can be described through the standard single-hit Poisson model of photosynthesis (Packer et al., 2011). Such model allows to evaluate the specific growth rate through normalization of the net carbon fixation rate of microalgae, P to the carbon content χ ($g_C\ g_{dw}^{-1}$) of the non lipidic fraction of microalgae. According to Packer et al. (2011) the value of χ is considered to remain constant during microalgal growth. Under these assumptions, the Liebig's law of the minimum for describing the specific growth rate of microalgae can be written as follows by modifying the formulation proposed by Packer et al. (2011) in order to take into account also iron limitation phenomena:

$$\mu = \min\left\{\mu_{\max}\left(1 - \frac{Q_{\mathrm{N}}^{\min}}{q_{\mathrm{N}}}\right); \mu_{\max}\left(1 - \frac{Q_{\mathrm{Fe}}^{\min}}{q_{\mathrm{Fe}}}\right); \frac{P}{\chi}\right\} \tag{14}$$

where the symbol significance is reported in the Notation. It is worth noting that iron and nitrogen quotas, namely q_{Fe} and q_{N}, vary with time according to the following ordinary differential equations (Cherif and Loreau, 2010):

$$\frac{dq_{\mathrm{Fe}}}{dt} = v_{\mathrm{Fe}} - \mu \cdot q_{\mathrm{Fe}} \tag{15}$$

$$\frac{dq_{\mathrm{N}}}{dt} = v_{\mathrm{N}} - \mu \cdot q_{\mathrm{N}} \tag{16}$$

along with the corresponding initial conditions:

$$q_{\mathrm{Fe}} = q_{\mathrm{Fe}}^0 \quad \text{at} \quad t = 0 \tag{17}$$

$$q_{\mathrm{N}} = q_{\mathrm{N}}^0 \quad \text{at} \quad t = 0 \tag{18}$$

where v_{Fe} and v_{N} represent the uptake rate of iron and nitrogen respectively, which, in turn depend upon the concentration of Fe and N available in the liquid bulk (i.e. in the growth medium) as well as upon the values of q_{Fe} and q_{N}. Specifically, the rate of iron uptake is related to the availability of Fe(III) in solution and is down-regulated by a linear satiation function of the cell quota q_{Fe} as cells approach their maximum allowed content of Fe (Ward et al., 2012):

$$v_{\mathrm{Fe}} = v_{\mathrm{Fe}}^{\max}\left(\frac{Q_{\mathrm{Fe}}^{\max} - q_{\mathrm{Fe}}}{Q_{\mathrm{Fe}}^{\max} - Q_{\mathrm{Fe}}^{\min}}\right) \cdot \frac{C_{\mathrm{Fe(III)}}}{K_{\mathrm{Fe}} + C_{\mathrm{Fe(III)}}} \tag{19}$$

where $C_{\mathrm{Fe(III)}}$ is the total mass concentration of Fe(III). From Eq. (19) it can be seen that the function expressing the cell satiation state, reported within parenthesis, is zero when the cell quota q_{Fe} is equal to its maximum allowed value $Q_{\mathrm{Fe}}^{\max}$, while it reaches one when q_{Fe} approaches the minimum allowed value $Q_{\mathrm{Fe}}^{\min}$ below which no cell

growth can take place. Such a function well describes the real behavior of microalgae cells which are capable to assimilate iron at a rate which increases as its internal content decreases. On the other hand, when the internal quota is maximum, microalgal cells activate specific mechanisms that prevent excessive accumulation of any type of nutrient by decreasing to zero the uptake rate (Ward et al., 2012).

When considering the nitrate uptake rate, it is worth mentioning that nitrates, once inside the algal cell, need to be reduced to nitrites and to ammonium in order to be used for protein synthesis. The reduction of nitrates is obtained through enzymatic reactions catalyzed by nitrate reductase whose activity is strongly influenced by iron availability within the cell. Specifically, nitrate reductase activity is enhanced by high iron availability within the cell (Ruangsomboon et al., 2013; Ward et al., 2012). Consequently, when iron cell quota is low, nitrates are not converted to nitrites so that cells, to prevent accumulation phenomena, reduce their uptake from the liquid bulk. Such effect of iron on nitrate uptake rate has been mathematically accounted for as follows (Ward et al., 2012):

$$v_N = v_N^{max}\left(\frac{Q_N^{max} - q_N}{Q_N^{max} - Q_N^{min}}\right)\cdot\frac{C_N}{K_N + C_N}\cdot\gamma_{Fe} \tag{20}$$

where γ_{Fe} is a normalized hyperbolic function that is equal to 0 when $q_{Fe} = Q_{Fe}^{min}$ and 1 when $q_{Fe} = Q_{Fe}^{max}$, respectively (Ward et al., 2012):

$$\gamma_{Fe} = \frac{q_{Fe} - Q_{Fe}^{min}}{Q_{Fe}^{max} - Q_{Fe}^{min}}\cdot\frac{Q_{Fe}^{max}}{q_{Fe}} \tag{21}$$

The net carbon fixation rate of microalgae through photosynthesis P, appearing in Eq. (14), has been evaluated as Poisson function of average light intensity (I_{av}) modified in order to take into account the dependence upon the iron quota of the initial slope of the photosynthesis–irradiance (P–I) curve, namely ($\beta\cdot\gamma_{Fe}$), and the chlorophyll-a cell quota q_{Chla} (Ward et al., 2012):

$$P = P_C^{sat}\cdot\left[1 - \exp\left(-\frac{\beta\cdot\gamma_{Fe}\cdot q_{Chla}\cdot I_{av}}{P_C^{sat}}\right)\right] \tag{22}$$

where P_C^{sat} represents the carbon-specific light-saturated photosynthetic rate which, according to Ward et al. (2012) can be written as:

$$P_C^{sat} = P_C^{max}\cdot\min\{\gamma_{Fe}, \gamma_N\} \tag{23}$$

where γ_N is expressed by:

$$\gamma_N = \frac{q_N - Q_N^{min}}{Q_N^{max} - Q_N^{min}} \tag{24}$$

The symbol significance is reported in the Notation. It is noteworthy that while the term β is known to be proportional to the product of the optical cross section of chlorophyll-a, a_{Chla} and the quantum efficiency φ, to the best of our knowledge, no information is available in the literature about its value for *C. vulgaris*.

Since the nitrogen uptake by algae leads to its consumption in the growth medium, the following mass balance can be written to describe the time evolution of its concentration in the bulk liquid phase of the batch system under investigation:

$$\frac{dC_N}{dt} = -v_N\cdot C_x \tag{25}$$

along with the initial condition

$$C_N = MW_N[NO_3^-]^0 \quad \text{at} \quad t = 0 \tag{26}$$

where $[NO_3^-]^0$ is the initial molar concentration of nitrates in the growth medium. In this regard it is worth mentioning that the material balances describing the evolution of iron species in the liquid bulk have been already reported in Eqs. (4)–(6). In Eq. (22) the term q_{Chla} is the amount of chlorophyll-a (Chla) per unit of microalgal biomass, namely the chlorophyll cell quota ($g_{Chla}\,g_{dw}^{-1}$). In this regard, it is important to highlight that the Chla content of algae can be modified as a result of photo-acclimation phenomena. Such a variation is affected by the availability of nitrogen and iron. Specifically, as the light intensity (I_{av}) in the culture decreases due to the increase of medium optical density, the algal cell is capable to synthesize "ex novo" new photosynthetic units (PSUs), containing chlorophyll-a, in order to better capture the incident photons (Strzepek et al., 2012). This acclimation mechanism allows the algae to adapt pigment (and especially chlorophyll) synthesis to light intensity (Bernard, 2011). Ultimately, in order to acclimate to the low light conditions, microalgae utilize a certain fraction of the assimilated nitrogen for synthesizing new molecules of Chla. Consequently, the synthesis rate of chlorophyll-a is strictly linked to the nitrogen uptake rate v_N and thus the mass balance for the chlorophyll cell quota can be then written as follows (Packer et al., 2011):

$$\frac{dq_{Chla}}{dt} = \theta_{Chla}^N\cdot v_N - \mu\cdot q_{Chla} \tag{27}$$

along with the initial condition:

$$q_{Chla} = q_{Chla}^0 \quad \text{at} \quad t = 0 \tag{28}$$

where θ_{Chla}^N ($g_{Chla}\,g_N^{-1}$) is the amount of chlorophyll-a that is synthesized for every weight unit of nitrogen assimilated by algae. Moreover, as recently reported in the literature (Strzepek et al., 2012), an increase of the PSUs number is coupled with the increase of the cellular concentrations of the iron-rich protein complexes that accomplish photosynthetic electron transport. Therefore, the process of chlorophyll synthesis consumes iron and is consequently affected by its availability within the cell. In the light of what above the amount of chlorophyll that is synthesized for every weight unit of nitrogen assimilated by algae, depends upon light intensity and iron availability within the cell, as follows (Ward et al., 2012):

$$\theta_{Chla}^N = \theta_{Chla}^{N,max}\cdot\left(\frac{P}{\beta\cdot\gamma_{Fe}\cdot q_{Chla}\cdot I_{av}}\right) \tag{29}$$

where $\theta_{Chla}^{N,max}$ is the maximum ratio at which nitrogen can be used for chlorophyll synthesis. In order to evaluate the average light intensity I_{av} within the culture, the conical volume of the flasks has been divided into infinitesimal volumes having height dz and a radius $R(z)$ which depends upon the same height. For each of these infinitesimal volumes the average light intensity has been evaluated according to Concas et al. (2012) as follows:

$$\bar{I}(z,t) = \frac{2\cdot I_0(t)}{R(z)\cdot\tau_a\cdot C_b(t)\cdot\pi}\left[1 - \int_0^{\frac{\pi}{2}}\cos(\omega)\cdot\exp(-2\cdot R(z)\cdot\tau_a\cdot C_b(t)\cdot\cos(\omega))\cdot d\omega\right] \tag{30}$$

where the symbol significance is reported in the Notation. Subsequently, in order to evaluate the average irradiance related to the entire culture volume of the flask (i.e. the conical volume), Eq. (30) was then integrated over z in the interval $0 < z < h$, where h is the height of the culture medium in the flask:

$$I_{av}(t) = \frac{\int_0^h \bar{I}(z,t)\cdot dz}{h} \tag{31}$$

The incident light intensity $I_0(t)$ appearing in Eq. (30), which varies with time as a square wave having amplitude equal to 100 $\mu E\,m^{-2}\,s^{-1}$ and a photoperiod T_p equal to 12 h, is evaluated as follows (cf. Concas et al., 2012):

$$\begin{cases} I_0(t) = 100(\mu E\ m^{-2}\ s^{-1}) & \text{if} \quad mod\left[\frac{int(t/T_p)}{2}\right] = 0 \\ I_0(t) = 0(\mu E\ m^{-2}\ s^{-1}) & \text{if} \quad mod\left[\frac{int(t/T_p)}{2}\right] \neq 0 \end{cases} \tag{32}$$

where the function "*int*" provides the integer part of the ratio (t/T_p), while the function "*mod*" gives the remainder of the division in its argument.

In order to quantitatively describe the lipid production by microalgae, it is assumed (cf. Jeffryes et al., 2013) that it can be either primary, i.e. directly related to metabolism and growth, or secondary, i.e. not coupled to cellular growth and typically occurring in response to a stress or external stimuli. Specifically, the material balance for lipid production can be expressed as follows (Jeffryes et al., 2013):

$$\frac{dC_\ell}{dt} = \alpha \cdot \frac{dC_x}{dt} + \eta \cdot C_x \tag{33}$$

along with the initial condition

$$C_\ell = q_\ell^0 C_b^0 \quad \text{at} \quad t = 0 \tag{34}$$

where q_ℓ^0 is the initial lipid content of biomass, C_b^0 is the initial concentration of the biomass including non-lipidic and lipidic fraction, while α ($g_{dw}\ g_{dw}^{-1}$) and η ($g_{dw}\ g_{dw}^{-1}\ min^{-1}$) represent the primary and secondary production rate, respectively. Therefore, the effect of iron can be twofold. In fact, while on one hand the high availability of iron allows algae to grow without nutrient limitation, on the other one, according to the experimental evidence, iron can trigger specific phenomena that lead to lipid accumulation. While such phenomena are still unclear, it is apparent that the extent of lipid accumulation in microalgae is positively correlated to iron concentration in solution (Liu et al., 2008; Yeesang and Cheirsilp, 2011; Ruangsomboon, 2012; Ruangsomboon et al., 2013). Thus, in this first attempt to model the effect of iron on lipid accumulation, we propose to set the non-growth associated production rate of lipids η as a linear function of the concentration of the bioavailable iron, i.e. $C_{Fe(III)}$ in the medium:

$$\eta = \eta_m C_{Fe(III)} \tag{35}$$

The total biomass concentration, C_b can be evaluated as the sum of the lipidic, C_ℓ and non-lipidic, C_x concentration of microalgae, while their lipid content at each cultivation time can be obtained as $q_\ell = C_\ell/C_b$.

The algorithm adopted to solve the mathematical model is schematically shown in the flowchart provided in the Supplementary material. The resulting system of ordinary differential equations was numerically integrated as an initial value problem by means of the subroutine DIVPAG of the International Mathematics and Statistics Libraries (IMSL) implemented in a computer code written in the Fortran programming language. The subroutine solves a system of first-order ordinary differential equations by using an implicit linear multistep method based on the exploitation of the fifth-order Gear's backward differentiation formulae (Gear, 1971). The integrals of Eqs. (30) and (31) were solved by invoking the IMSL subroutine DQDAWO which takes advantage of either a modified Clenshaw–Curtis procedure or a Gauss–Kronrod 7/15 rule to approximate the integral on a specific subinterval (Piessens et al., 1983). Finally, in order to fit the experimental data, tuning of model parameters values was carried out through an optimization procedure written in the Fortran language which minimizes an objective function based on the least-squares method. It should be noted that when no iron is added to the solution, in the comprehensive model described above Eqs. (4)–(11) should not be taken into account. In addition under such experimental conditions $v_{Fe} = 0$ and $\eta = 0$.

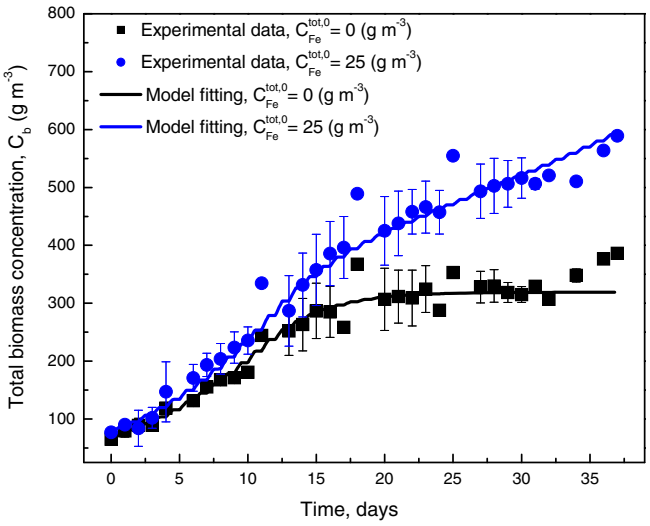

Fig. 2. Comparison between model results (fitting) and experimental data in terms of total biomass concentration, which accounts for both non lipidic and lipidic fraction, as a function of time when the initial concentration of total dissolved iron is equal to 0 and 25 g m^{-3}, respectively.

4. Results and discussion

The effect of iron concentration on the growth kinetics of *C. vulgaris* and its lipid content was quantitatively interpreted in this work. In order to demonstrate the reliability of the proposed model, the corresponding results were compared with suitable experimental data. To this aim, specific experiments were carried out by cultivating *C. vulgaris* in batch stirred flasks where the initial concentration of dissolved iron was suitably changed. Specifically, the growth and lipid accumulation kinetics in absence of iron was first investigated. Subsequently, further experiments were carried out to evaluate the effect of the initial concentration of dissolved inorganic iron on the growth of *C. vulgaris* by varying the initial concentration of $FeSO_4{\cdot}7H_2O$ and $Na_2EDTA{\cdot}2H_2O$, while keeping fixed their molar ratio (i.e. $[FeSO_4{\cdot}7H_2O]/[Na_2EDTA{\cdot}2H_2O]$). In Fig. 2 the time evolution of total biomass concentration obtained when cultivating *C. vulgaris* in absence of dissolved iron is shown. In particular, it can be observed that the culture starts growing without showing a significant lag phase despite the absence of iron in solution. This behavior justifies the choice of avoiding the use of a classical Monod approach to simulate microalgal growth. In fact the Monod model would have clearly failed in simulating the data reported in Fig. 2 since, accordingly to such model, growth rate of *C. vulgaris* should have been equal to zero in absence of dissolved iron. On the contrary, according to the model adopted, microalgae can grow also when iron concentration in solution is zero by exploiting the intracellular reservoir of iron, namely the initial iron cell quota. Thus, the initial intracellular content of iron was high enough to permit *C. vulgaris* cells to grow and duplicate for a specific time interval, as shown in Fig. 2. In fact, it can be observed that culture grows until about 10 days, while after 20 days of cultivation it reaches a sort of "plateau" when the biomass concentration is about 320 g m^{-3}.

Such stationary phase is reached due to the consumption of the available intracellular iron. This aspect is properly taken into account in Eq. (15) which states that, since the uptake of iron v_{Fe} is zero because no iron is added to the solution, the iron cell quota q_{Fe} correspondingly decreases, as it may be clearly observed from Fig. 3a. Therefore, when the iron cell quota reaches the minimum value that allows microalgae growth, namely Q_{Fe}^{min}, the culture stops growing (cf. Fig. 3a). It is worth noting that the experiment

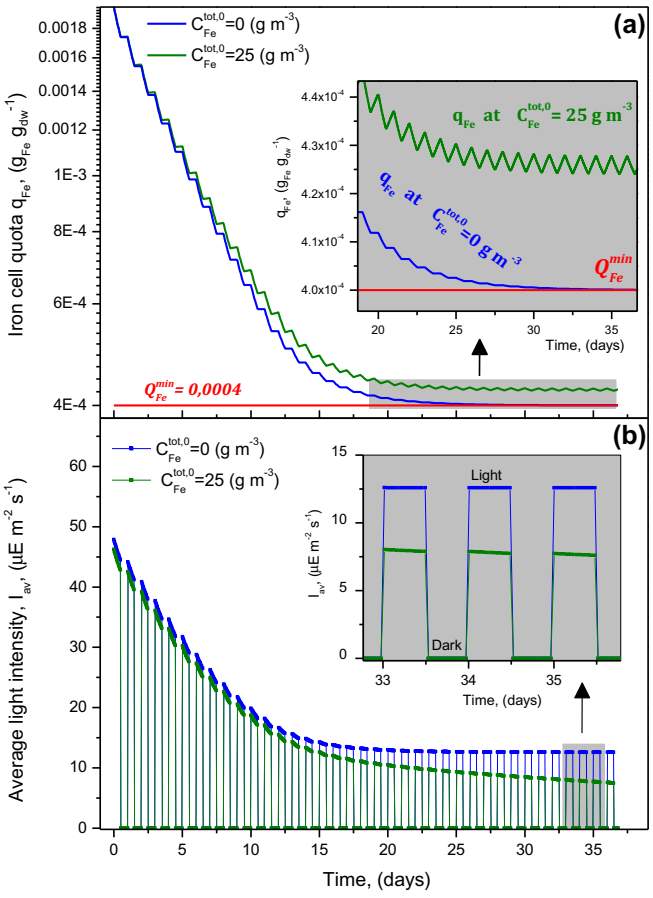

Fig. 3. Time evolution of iron cell quota (a) and average light intensity (b) when the initial concentration of total dissolved iron is equal to 0 and 25 g m^{-3}, respectively, as simulated by the proposed model.

carried out in absence of dissolved iron permits to suitably evaluate the initial cell quota of iron, q_{Fe}^0. In fact, since no iron was present in solution and growth ends when the cell quota is equal to Q_{Fe}^{min}, from a simple material balance related on iron it follows that $q_{Fe}^0 = (C_x^f \cdot Q_{Fe}^{min})/C_x^0$, where C_x^0 and C_x^f are the initial and the final concentrations of the non lipidic biomass concentration, respectively. The obtained value of the initial iron cell quota is reported in Table 2, where the other model parameters used for the simulations are also summarized.

All the model parameters values appearing in Table 2 are taken from the literature except for the initial slope of the iron-dependent photosynthesis irradiance (P–I) curve β, the maximum iron uptake rate v_{Fe}^{max} as well as the maximum rate of secondary (iron induced) production of lipids η_m which have been suitably tuned through a nonlinear fitting procedure in order to quantitatively interpret the experimental data. Specifically, their values are obtained through direct comparison, based on the least squares methodology, of model results with experimental data in terms of biomass concentration evolution during microalgal growth as well as of lipid content at the end of cultivation. In particular, it is important to note that the only parameter which was tuned to fit the experimental data of Fig. 2 and the corresponding final lipid content of Fig. 4, was β since, in absence of dissolved iron, the model does not require the knowledge of the values of v_{Fe}^{max} and η_m. In this regard it is also worth mentioning that the value of the parameter α, i.e. the primary rate of lipid production, was evaluated on the basis of the experimental results obtained in absence of iron, where the initial lipid content of microalgae (q_ℓ^0) was equal to the one observed at the end of the cultivation experiment (q_ℓ^f). Such experimental result suggests that in absence of iron the primary rate of lipid production is such that the ratio between lipids concentration C_ℓ and total biomass concentration of microalgae, i.e. $C_\ell + C_x$, remains constant during cultivation and specifically equal to the value of q_ℓ^0. Under such conditions the value of α can be evaluated as $q_\ell^0/(1 - q_\ell^0)$ according to what shown in the Appendix. Therefore, since the value of q_ℓ^0 was experimentally measured, α can be easily evaluated and used for simulations.

In Fig. 2, the comparison between experimental data and model fitting is also shown. The relative error obtained by the fitting procedure is equal to 6.2% while the value of β results to be 1.05×10^{-3} (g_C m^2 g_{Chla}^{-1} μE^{-1}). From Fig. 2 it might be observed that the proposed model quantitatively captures the growth trends

Table 2
Model parameters.

Symbol	Value	Units	Reference
k_d (at ph = 8)	6.0×10^{-5}	min^{-1}	Hudson et al. (1990)
k_f	1.2	m^3 mol_{EDTA}^{-1} min^{-1}	Hudson et al. (1990)
k_{Fe}	9.5×10^{-3}	g_{Fe} m^{-3}	Calculated from Ward et al. (2012)
k_{hv} (at 95 μE m^{-2} s^{-1})	1.02×10^{-4}	min^{-1}	Hudson et al. (1990)
k_N	1.9×10^{1}	g_N m^{-3}	Concas et al. (2012)
k_{ox}	6.0×10^{-1}	min^{-1}	Hudson et al. (1990)
p_c^{max}	2.4×10^{-4}	g_C g_{dw}^{-1} min^{-1}	Yoo et al. (2010)
q_{Chla}^0	1.2×10^{-2}	g_{Chla} g_{dw}^{-1}	Piorreck et al. (1984)
q_{Fe}^0	2.0×10^{-3}	g_{Fe} g_{dw}^{-1}	Evaluated as reported in the text
Q_{Fe}^{max}	5.5×10^{-3}	g_{Fe} g_{dw}^{-1}	Mandalam and Palsson (1998)
Q_{Fe}^{min}	4.0×10^{-4}	g_{Fe} g_{dw}^{-1}	Mandalam and Palsson (1998)
q_ℓ^0	9.6×10^{-2}	g_{dw} g_{dw}^{-1}	Experimentally evaluated
q_ℓ^f at (C_{Fe} = 0)	9.6×10^{-2}	g_{dw} g_{dw}^{-1}	Experimentally evaluated when no iron is added in solution
q_N^0	7.7×10^{-2}	g_N g_{dw}^{-1}	Evaluated as reported in the text
Q_N^{max}	7.7×10^{-2}	g_N g_{dw}^{-1}	Mandalam and Palsson (1998)
Q_N^{min}	6.2×10^{-2}	g_N g_{dw}^{-1}	Mandalam and Palsson (1998)
v_{Fe}^{max}	5.5×10^{-9}	g_{Fe} g_{dw}^{-1} min^{-1}	Tuned parameter
v_N^{max}	3.09×10^{-5}	g_N g_{dw}^{-1} min^{-1}	Evaluated from Bernard (2011)
α	1.06×10^{-1}	g_{dw} g_{dw}^{-1}	Experimentally evaluated
β	1.05×10^{-3}	g_C m^2 g_{Chla}^{-1} μE^{-1}	Tuned parameter
χ	6.1×10^{-1}	g_C g_{dw}^{-1}	Packer et al. (2011)
η_m	1.11×10^{-7}	g_{dw} m^3 g_{dw}^{-1} min^{-1} g_{Fe}^{-1}	Tuned parameter
μ_{max}	1.07×10^{-3}	min^{-1}	Concas et al. (2012)
$\theta_{Chla}^{N,max}$	5.7×10^{-1}	g_{Chla} g_N^{-1}	Bernard (2011)
τ_a	4.35×10^{-1}	m^2 g^{-1}	Concas et al. (2012)

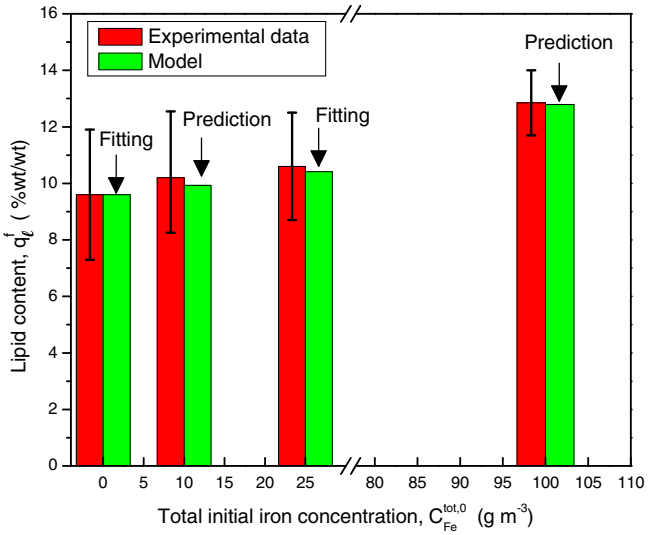

Fig. 4. Comparison between model results (fitting/prediction) and experimental data in terms of final lipid content of microalgae as a function of the initial concentration of total dissolved iron.

from day to day in absence of iron. The "oscillating" behavior of model displayed in Fig. 2 is due to the fact that, in absence of light, photosynthesis phenomena do not take place and thus biomass concentration does not increase during this time period.

In order to evaluate the effect of iron on microalgae growth rate and lipid accumulation further experiments were performed by setting the initial concentration of $FeSO_4{\cdot}7H_2O$ equal to 4.5×10^{-1} mol m^{-3} and the initial concentration of $Na_2EDTA{\cdot}2H_2O$ to 4.0×10^{-1} mol m^{-3}, thus assuring a molar ratio between iron and EDTA equal to 1.12:1. The corresponding initial concentration of total iron in solution, i.e. $C_{Fe}^{tot,0}$, was thus 25 g_{Fe} m^{-3}. From the analysis of experimental data shown in Fig. 2 it can be observed that under such operating conditions the culture keeps growing during the whole investigated time interval. Consequently, the biomass concentration at the end of the experiment is almost doubled with respect to the corresponding one observed in the case of absence of iron. Such a behavior is due to the fact that microalgae can prevent the decrease of their iron cell quota by taking advantage of iron available in solution. Therefore, as it might be observed from Fig. 3a, the cell quota remains always greater than the minimum value Q_{Fe}^{min} as a result of the uptake of iron from solution. In Fig. 2, the comparison between experimental data and model fitting, for the case where $C_{Fe}^{tot,0}$ is equal to 25 g_{Fe} m^{-3}, is also shown. In this case the values of β obtained as above reported was kept fixed while the kinetic parameters v_{Fe}^{max} and η_m were suitably tuned in order to fit the experimental data obtained in the presence of iron, i.e. using both the experimental data shown in Fig. 2 and Fig. 4 corresponding to a total initial iron concentration of 25 g_{Fe} m^{-3}.

The relative error obtained by the fitting procedure is equal to about 6% while the fitted values of v_{Fe}^{max} and η_m were 5.5×10^{-9} (g_{Fe} g_{dw}^{-1} min^{-1}) and 1.11×10^{-7} (g_{dw} m^3 g_{dw}^{-1} min^{-1} g_{Fe}^{-1}), respectively. It should be also noted that the obtained value of v_{Fe}^{max} is consistent with the wide range of values of maximum iron uptake rates available in the literature, even if obtained when considering different algal strains (Ward et al., 2012; Buitenhuis and Geider, 2010; Hudson et al., 1990). As it can be observed from Fig. 2, the experimental behavior is well captured by the proposed model also in terms of the change of the slope of the growth curve which is due to the fact that, under iron-replete conditions, at the start of the experiment, nitrogen becomes the main limiting nutrient and thus the value of the growth rate is dictated by nitrogen cell quota (cf. Eq. (14)). However, as the culture grows, its optical density increases and consequently, as shown in Fig. 3b, the light intensity that is available for microalgae, decreases. As a result the carbon specific photosynthetic rate, P decreases according to Eq. (22) so that when very low values are reached, the culture becomes light-limited instead of nitrogen-limited and consequently the variation law of the growth rate changes according to Eq. (14). This phenomenon provokes the change in the slope of the growth curve related to the experiment with $C_{Fe}^{tot,0} = 25$ g m^{-3} observed in Fig. 2 after 15 days of cultivation.

From Fig. 3 it can be seen that also the final lipid content is well fitted by the proposed model when total initial iron concentration in solution is equal to 25 g_{Fe} m^{-3}. Moreover, the experimental data confirm that total lipid content increases when the iron concentration in solution is augmented. Specifically, the lipid content increased from 9.6% to 10.6% by dry weight when the total initial iron concentration in solution was increased from 0 to 25 g_{Fe} m^{-3}, respectively. These results are qualitatively consistent with the ones obtained by Liu et al. (2008) using a marine strain of *C. vulgaris*. In fact also in this case, a simultaneous increase of growth rate and lipid content was observed when iron concentration in solution was augmented. However, from a quantitative point of view, a less pronounced increase of lipid content is observed in our work with respect to the corresponding one obtained by Liu et al. (2008), where the lipid content increased from 0% to about 57% when the initial iron concentration was augmented from 0 to 6×10^{-1} g m^{-3}, respectively. The differences with the present results are probably due to several reasons. First, all data published by Liu et al. (2008) refer to a marine strain of *C. vulgaris*, while in the present work we took advantage of a freshwater strain. Moreover, different growth media were used and different illumination conditions were adopted. In particular, it is interesting to note that, in the work by Liu et al. (2008), $FeCl_3$ was employed as source of iron instead of $FeSO_4$. Thus, the iron addition is coupled to the presence of chloride species which is well known to provoke oxidative stress that is, in turn, capable to trigger lipid accumulation phenomena in microalgae. Therefore, the effect on lipid accumulation due to the presence of chloride species was probably superimposed to the one related to iron when considering the experiments performed by Liu et al. (2008).

Fig. 5 shows the time evolution of iron-related species as simulated by the proposed model when $C_{Fe}^{tot,0}$ is set equal to 25 g m^{-3}. In this figure, the log scale is adopted for the time axis to allow the reader to better appreciate the dynamics of iron speciation

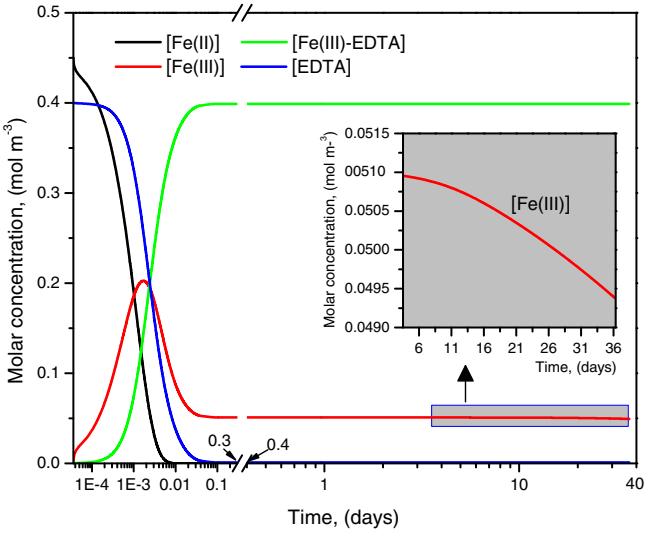

Fig. 5. Time evolution of different iron species in solution as simulated by the proposed model when the initial concentration of total dissolved iron is equal to 25 g m^{-3}.

phenomena taking place during the first 0.3 days of the experiments. In fact, since the reactions accounted for in Fig. 1 are characterized by high rates, they are almost completed within about 0.3 days. As it can be observed, after this period of time, most of the iron in solution is bonded to EDTA which serves as a buffering agent. Simultaneously, the concentration of Fe(III), i.e. the useful form of iron for algae, increases until it reaches 0.06 mol m^{-3} at about 0.3 days while subsequently it does not vary significantly as a result of the uptake by algae. This is due to the fact that Fe(III) concentration is much higher than the minimum needed by algae to grow. Consequently, the uptake of iron by algae does not result in lowering of Fe(III) concentration as it might be appreciated at the scale adopted. However, when zooming on a more detailed scale (cf. grey box in Fig. 5), the reduction of Fe(III) concentration due to iron uptake by algae, may be clearly seen. It is important to remark here that such iron concentrations have been adopted in order to trigger lipid accumulation. In fact, while the iron starvation phenomena can be avoided by using much lower concentrations of iron, in order to provoke the oxidative phenomena that represent the basis for lipid accumulation, high concentrations of iron are needed.

Finally, to test the predictive model capability, the experimental data obtained when cultivation was carried out by starting with total iron concentration equal to 10 and 100 g_{Fe} m^{-3}, respectively, were simulated. The corresponding initial EDTA concentrations were set in order to assure always the same initial molar ratio between iron and EDTA. Model parameters used in these simulation runs are the same as reported in Table 2. It is important to remark that in this case no parameter has been adjusted. The comparison between model predictions and experimental data is shown in Fig. 3 for the case of final lipid content and in Fig. 6 in terms of biomass concentrations as a function of time. As it can be seen, the proposed model predicts the experimental behavior both in terms of biomass concentration and final lipid content with sufficient accuracy when varying the initial total concentration of iron. In particular from Fig. 6 one can observe that, under such operating conditions, microalgae grow in a similar way. In fact the biomass concentration achieved at the end of the experiment carried out when using an iron concentration of 100 g m^{-3} was clearly higher than the corresponding one obtained when using lower iron concentrations. Ultimately, when the iron concentration is augmented beyond 10 g m^{-3}, a slight increase in the total biomass growth rate is also observed. Such a behavior is consistent with the data reported in the literature (Liu et al., 2008; Yeesang and Cheirsilp, 2011; Mata et al., 2013; Ruangsomboon et al., 2013), where it is shown that when iron is added beyond a certain value a slight increase in the growth rate can be detected while, on the contrary, the lipid content results to be clearly augmented.

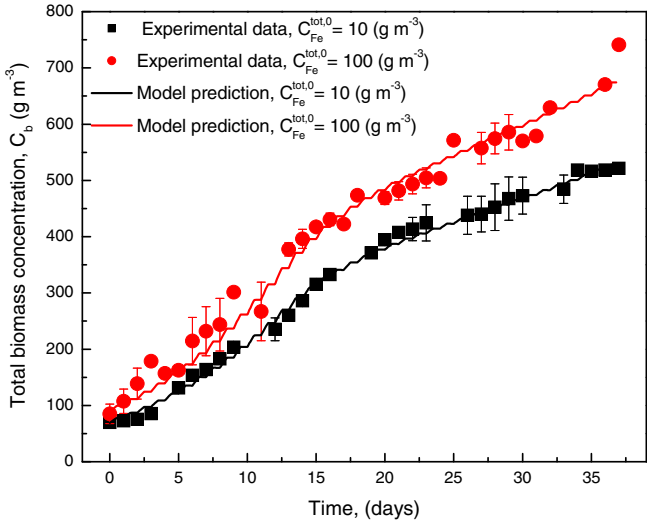

Fig. 6. Comparison between model results (prediction) and experimental data in terms of total biomass concentration, which accounts for both non lipidic and lipidic fraction, as a function of time when the initial concentration of total dissolved iron is equal to 10 and 100 g m^{-3}, respectively.

While the proposed model well captures such experimental behavior, the phenomena involved in the iron-induced lipid accumulation in *C. vulgaris* are still unclear. On the basis of the literature data, only some hypotheses can be formulated about the mechanism that underlies the increased lipid accumulation deriving from the augmentation of iron concentration in solution. A first hypothesis is based on the fact that, under illumination, iron can promote the generation of hydroxyl and superoxide radicals that may subject the cells to a significant oxidative stress (Fujii et al., 2010). Nevertheless, several micro algae have the ability to produce relatively high amounts of storage lipids as a response to oxidative stress (Sakthivel et al., 2011). In particular it has been recently demonstrated that specific intracellular content of lipids of *C. vulgaris* is positively correlated to the intracellular concentration of free radicals in a power law fashion (Menon et al., 2013). Thus the increased concentration of iron in solution might have led to an increased production of free radicals, both outside and inside the cell, which, in turn, might have stimulated the microalgal cells to synthesize more lipids. In addition, as discussed for soybeans seeds by Plank et al. (2001), iron can play an important role in activating the enzyme acetyl-CoA carboxylase (ACCase) which may, in turn, catalyze the rate-limiting step in the bio-synthesis of fatty acids. While specific experiments should be performed to confirm such effects of iron on microalgae, a similar mechanism might be assumed to occur in *C. vulgaris*. Moreover, the two mechanisms discussed above are probably acting simultaneously. In addition, according to Menon et al. (2013), also the high concentration of radicals, which is somehow related to the presence of iron, is capable to enhance the activity of ACCase in *C. vulgaris* by accelerating the irreversible carboxylation of acetyl-CoA to malonyl-CoA. However, all the hypotheses above need to be confirmed through specific experiments. Work is on the way along these lines.

5. Concluding remarks

A comprehensive mathematical model for the simulation of the effect of dissolved iron on the growth and lipid accumulation of *C. vulgaris*, is proposed in this work. By comparing model results with experimental data a good matching is obtained. Moreover, the experimental results have shown that a simultaneous increase of the growth rate and lipid content of *C. vulgaris* can be achieved by increasing the dissolved iron concentration within a specific range. Therefore, the mathematical model might permit to identify the iron concentrations that optimize the lipid productivity of *C. vulgaris* in batch photobioreactors.

Acknowledgements

One of us (A. S.) gratefully acknowledges Sardinia Regional Government for the financial support of his PhD scholarship (P.O.R. Sardegna F.S.E. Operational Programme of the Autonomous Region of Sardinia, European Social Fund 2007–2013 - Axis IV Human Resources, Objective l.3, Line of Activity l.3.1).

Appendix A

In the absence of iron in solution, since the lipid content of microalgae remains constant during microalgal growth, the lipid cell quota can be evaluated as follows:

$$q_\ell = \frac{C_\ell}{C_x + C_\ell} = q_\ell^0 \tag{A.1}$$

Consequently, we obtain that:

$$C_\ell = \frac{q_\ell^0}{1 - q_\ell^0} \cdot C_x \tag{A.2}$$

and, by differentiating in the time variable the equation above, it follows that:

$$\frac{dC_\ell}{dt} = \left(\frac{q_\ell^0}{1 - q_\ell^0}\right) \frac{dC_x}{dt} \tag{A.3}$$

Therefore, since in absence of iron in solution, Eq. (33) can be written as:

$$\frac{dC_\ell}{dt} = \alpha \frac{dC_x}{dt} \tag{A.4}$$

it clearly follows that:

$$\alpha = \frac{q_\ell^0}{1 - q_\ell^0} \tag{A.5}$$

Appendix B. Supplementary data

Supplementary data associated with this article can be found, in the online version, at http://dx.doi.org/10.1016/j.biortech.2013.11.085.

References

Baky, H.H.A.E., El-Baroty, G.S., Bouaid, A., Martinez, M., Aracil, J., 2012. Enhancement of lipid accumulation in Scenedesmus obliquus by Optimizing CO_2 and Fe^{3+} levels for biodiesel production. Bioresour. Technol. 119, 429–432.

Bernard, O., 2011. Hurdles and challenges for modelling and control of microalgae for CO2 mitigation and biofuel production. J. Process Control 21, 1378–1389.

Buitenhuis, E.T., Geider, R.J., 2010. A model of phytoplankton acclimation to iron–light colimitation. Limnol. Oceanogr. 55, 714–724.

Cheize, M., Sarthou, G., Croot, P.L., Bucciarelli, E., Baudoux, A.-C., Baker, A.R., 2012. Iron organic speciation determination in rainwater using cathodic stripping voltammetry. Anal. Chim. Acta 736, 45–54.

Cherif, M., Loreau, M., 2010. Towards a more biologically realistic use of Droop's equations to model growth under multiple nutrient limitation. Oikos 119, 897–907.

Concas, A., Pisu, M., Cao, G., 2010. Novel simulation model of the solar collector of BIOCOIL photobioreactors for CO_2 sequestration with microalgae. Chem. Eng. J. 157, 297–303.

Concas, A., Lutzu, G.A., Pisu, M., Cao, G., 2012. Experimental analysis and novel modeling of semi-batch photobioreactors operated with *Chlorella vulgaris* and fed with 100%(v/v) CO_2. Chem. Eng. J. 213, 203–213.

Concas, A., Lutzu, G.A., Locci, A.M., Cao, G., 2013. Nannochloris eucaryotum growth in batch photobioreactors: kinetic analysis and use of 100% (v/v) CO_2. Adv. Env. Res. 2, 19–33.

Fujii, M., Rose, A.L., Omura, T., Waite, T.D., 2010. Effect of Fe(II) and Fe(III) transformation kinetics on iron acquisition by a toxic strain of *Microcystis aeruginosa*. Environ. Sci. Technol. 44, 1980–1986.

Gear, C.W., 1971. Numerical Initial Value Problems in Ordinary Differential Equations. Prentice-Hall, Englewood Cliffs, New Jersey.

Gerringa, L., De Baar, H., Timmermans, K., 2000. A comparison of iron limitation of phytoplankton in natural oceanic waters and laboratory media conditioned with EDTA. Mar. Chem. 68, 335–346.

Hudson, R.J., Morel, F.M., Morel, F., 1990. Iron transport in marine phytoplankton: Kinetics of cellular and medium coordination reactions. Limnol. Oceanogr. 35, 1002–1020.

Jeffryes, C., Rosenberger, J., Rorrer, G.L., 2013. Fed-batch cultivation and bioprocess modeling of Cyclotella sp. for enhanced fatty acid production by controlled silicon limitation. Algal Res. 2, 16–27.

Liu, Z.-Y., Wang, G.-C., Zhou, B.-C., 2008. Effect of iron on growth and lipid accumulation in *Chlorella vulgaris*. Bioresour. Technol. 99, 4717–4722.

Mandalam, R.K., Palsson, B., 1998. Elemental balancing of biomass and medium composition enhances growth capacity in high-density *Chlorella vulgaris* cultures. Biotechnol. Bioeng. 59, 605–611.

Mata, T.M., Almeida, R., Caetano, N.S., 2013. Effect of the culture nutrients on the biomass and lipid productivities of microalgae *Dunaliella tertiolecta*. Chem. Eng. Trans. 32, 973–978.

Menon, K.R., Balan, R., Suraishkumar, G., 2013. Stress induced lipid production in *Chlorella vulgaris*: relationship with specific intracellular reactive species levels. Biotechnol. Bioeng. 110, 1627–1636.

Millero, F.J., Yao, W., Aicher, J., 1995. The speciation of Fe(II) and Fe(III) in natural waters. Mar. Chem. 50, 21–39.

Molina Grima, E., Robles Medina, A., Giménez Giménez, A., Sánchez Pérez, J.A., Garcia Camacho, F., García Sánchez, J.L., 1994. Comparison between extraction of lipids and fatty acids from microalgal biomass. J. Am. Oil Chem. Soc. 71, 955–959.

Morgan, B., Lahav, O., 2007. The effect of pH on the kinetics of spontaneous Fe(II) oxidation by O2 in aqueous solution–basic principles and a simple heuristic description. Chemosphere 68, 2080–2084.

Packer, A., Li, Y., Andersen, T., Hu, Q., Kuang, Y., Sommerfeld, M., 2011. Growth and neutral lipid synthesis in green microalgae: a mathematical model. Bioresour. Technol. 102, 111–117.

Piessens, R., deDoncker-Kapenga, E., Uberhuber, C.W., Kahaner, D.K., 1983. QUADPACK. Springer-Verlag, New York.

Piorreck, M., Baasch, K.-H., Pohl, P., 1984. Biomass production, total protein, chlorophylls, lipids and fatty acids of freshwater green and blue-green algae under different nitrogen regimes. Phytochemistry 23, 207–216.

Plank, D.W., Gengenbach, B.G., Gronwald, J.W., 2001. Effect of iron on activity of soybean multi-subunit acetyl-coenzyme A carboxylase. Physiol. plantarum 112, 183–194.

Quinn, J., de Winter, L., Bradley, T., 2011. Microalgae bulk growth model with application to industrial scale systems. Bioresour. Technol. 102, 5083–5092.

Ruangsomboon, S., 2012. Effect of light, nutrient, cultivation time and salinity on lipid production of newly isolated strain of the green microalga, *Botryococcus braunii* KMITL 2. Bioresour. Technol. 109, 261–265.

Ruangsomboon, S., Ganmanee, M., Choochote, S., 2013. Effects of different nitrogen, phosphorus, and iron concentrations and salinity on lipid production in newly isolated strain of the tropical green microalga, Scenedesmus dimorphus KMITL. J. Appl. Phycol. 25, 867–874.

Sakthivel, R., Sanniyasi, E., Arif, M.M., 2011. Microalgae lipid research, past, present: a critical review for biodiesel production, in the future. J. Exp. Sci. 2, 29–49.

Scott, S.A., Davey, M.P., Dennis, J.S., Horst, I., Howe, C.J., Lea-Smith, D.J., Smith, A.G., 2010. Biodiesel from algae: challenges and prospects. Curr. Opin. Biotechnol. 21, 277–286.

Shaked, Y., Kustka, A.B., Morel, F.M., 2005. A general kinetic model for iron acquisition by eukaryotic phytoplankton. Limnol. Oceanogr. 50, 872–882.

Sharma, K.K., Schuhmann, H., Schenk, P.M., 2012. High lipid induction in microalgae for biodiesel production. Energies 5, 1532–1553.

Strzepek, R.F., Hunter, K.A., Frew, R.D., Harrison, P.J., Boyd, P.W., 2012. Iron-light interactions differ in Southern Ocean phytoplankton. Limnol. Oceanogr. 57, 1182–1200.

Ward, B.A., Dutkiewicz, S., Jahn, O., Follows, M.J., 2012. A size-structured food-web model for the global ocean: web appendix:ecosystem model structure. Limnol. Oceanogr. 57, 1877–1891.

Yeesang, C., Cheirsilp, B., 2011. Effect of nitrogen, salt, and iron content in the growth medium and light intensity on lipid production by microalgae isolated from freshwater sources in Thailand. Bioresour. Technol. 102, 3034–3040.

Yoo, C., Jun, S.-Y., Lee, J.-Y., Ahn, C.-Y., Oh, H.-M., 2010. Selection of microalgae for lipid production under high levels carbon dioxide. Bioresour. Technol. 101, S71–S74.